and

$$\alpha \approx \beta_0(1+2/[1+(\omega\tau_\epsilon)^2]). \quad (2)$$

This approximation possesses the correct high- and low-frequency limits, β_0 and $3\beta_0$, respectively, and with a reasonable choice of τ_ϵ should be sufficiently good at intermediate frequencies. To determine an appropriate value for the relaxation time we have calculated the increase in average electron energy $\bar{x}$ from the numerical solution for the dc case and have defined τ_ϵ by the equation

$$dx/dt=\mu eE^2/kT=\bar{x}/\tau_\epsilon. \quad (3)$$

The values obtained for $\omega\tau_\epsilon$ by this procedure at 10-kMc/sec range from 0.15 at 300° to about 9.2 at 77° with only slight impurity dependence. The ratio of these values to $\omega\tau_p$ for momentum scattering is about 10 at 300° and over 60 at 77°K. We have applied this analysis to the three samples of Figs. 1 and 2 and have plotted the results in Fig. 3. Curves I–A through I–D show the frequency dependence of sample I. I–A and I–B are the values of α at the high and low frequency limits respectively, and I–C and I–D give the transitions between these two limits at 8.2 and 12.0 kMc/sec.

Although the agreement between theory and experiment could have been improved slightly by minor adjustments of the two available parameters, we feel that the existing agreements substantiate to a considerable extent the assumptions made and that the discrepancies reflect fundamental omissions from the scattering theory. It appears probable that an adequate description of impurity effects in transport theory of semiconductors will require a more elaborate model.

ACKNOWLEDGMENTS

The authors wish to thank the many members of the IBM Research Organization who have contributed to this investigation, with special thanks to Dr. P. J. Price for many stimulating discussions.

PHYSICAL REVIEW VOLUME 137, NUMBER 5A 1 MARCH 1965

Some Transport Properties of Oxygen-Deficient Single-Crystal Potassium Tantalate ($KTaO_3$)

S. H. WEMPLE
Bell Telephone Laboratories, Murray Hill, New Jersey
(Received 6 October 1964)

Hall-effect and electrical-conductivity measurements have been made on reduced single crystals of the perovskite potassium tantalate ($KTaO_3$) over the temperature range 1.6–295°K. Lattice scattering predominates above 100°K where the Hall mobility satisfies the empirical expression $\mu_H=8\times10^8T^{-3}$ cm²/V-sec. The room-temperature value is 30 cm²/V-sec. Below 100°K, ionized donor and impurity scattering become important, although mobilities as large as 23 000 cm²/V-sec have been observed at 4.2°K. These results are compared with published data for the 3*d* band in isostructural $SrTiO_3$ and shown to be consistent with the expected larger overlap of 5*d* orbitals. Free-carrier optical-absorption measurements presented in this paper indicate that electron scattering at room temperature in $KTaO_3$ is mainly by the highest frequency longitudinal polar mode situated at approximately 0.12 eV. Dielectric-constant measurements have also been made. These data show an extrapolated Curie temperature of 4±2°K for $KTaO_3$ with nonferroelectric behavior at 1.6°K.

INTRODUCTION

ELECTRON transport in many transition-metal oxides is thought to occur in "bands" derived from cation *d* orbitals.[1–4] Depending upon the extent of *d*-orbital overlap in the crystal lattice, the appropriate conduction model appears to range from a conventional Bloch band to localized orbital "hopping" as in the vanadium spinels.[2] Recently, Kahn *et al.*[5] performed tight binding band calculations on several titanates, i.e., rutile (TiO_2) and the perovskites $SrTiO_3$ and $BaTiO_3$. The theoretical results suggest that a relatively narrow, high effective mass many-valley conduction band formed primarily from titanium 3*d* orbitals exists in these materials. Published transport data[5–13] are in

[1] N. B. Hannay, *Semiconductors* (Reinhold Publishing Corporation, New York, 1959).
[2] D. B. Rogers, R. J. Arnott, A. Wald, and J. B. Goodenough, Chem. Phys. Solids 24, 347 (1963).
[3] J. Yamashita, J. Appl. Phys. 32, 2215 (1961).
[4] J. Yamashita and T. Kurosawa, J. Phys. Soc. Japan 15, 802 (1960).
[5] A. H. Kahn, P. R. Frederikse, and J. H. Becker, paper presented at Buhl International Conference on Transition Metal Compounds, 31 October–1 November 1963, Carnegie Institute of Technology, Pittsburgh, Pennsylvania (unpublished).
[6] H. P. R. Frederikse, W. R. Thurber, and W. R. Hosler, Phys. Rev. 134, A442 (1964).
[7] R. G. Breckenridge and W. R. Hosler, Phys. Rev. 91, 793 (1953).
[8] G. A. Acket and J. Volgler, Physica 29, 225 (1963).
[9] S. V. Bogdanov and V. A. Rossuskin, Bull. Acad. Sci. USSR, Phys. Ser. 24, 1248 (1960).
[10] H. P. R. Frederikse, W. R. Hosler, and J. H. Becker, *Proceedings of the International Conference on Semiconductor Physics, Exeter* (The Institute of Physics and the Physical Society, London, 1960), p. 868.
[11] F. A. Grant, Rev. Mod. Phys. 31, 646 (1959).
[12] G. Rupprecht, W. Winter, and J. S. Waugh, Report S-452, Contract No. AF 30-602-2678, Raytheon Company, Waltham, Massachusetts (unpublished).
[13] K. Kawabe and Y. Inuishi, Japan J. Appl. Phys. 2, 793 (1963).

qualitative agreement with this conclusion although the observed mobility temperature dependence as well as the free-carrier-absorption data have not been explained. It was felt worthwhile therefore to examine transport properties of transition metal oxides belonging to the $4d$ or $5d$ series. Kofstad[14–16] and others[17–18] have studied $4d$ and $5d$ oxides to a limited extent as part of defect-structure investigations, but Hall measurements are not available. Morin,[19] and more recently Nelson,[20] have suggested that electron mobilities in d-band semiconductors should tend to increase with increasing principle quantum number n simply because the nd wave functions tail off less rapidly as n increases.

In this paper we present some transport properties of the perovskite $KTaO_3$ in which conduction is presumably in a $5d$ band associated with the tantalum ions. This material is in many ways similar to $SrTiO_3$ so that comparison of our results with those recently reported by Frederikse, Thurber, and Hosler[6] on $SrTiO_3$ should be meaningful. The donors which give rise to n-type conduction in all samples of $KTaO_3$ are probably oxygen vacancies although a defect structure study has not been attempted. Data presented in this paper include electrical conductivity and Hall-effect measurements over the temperature range 1.6–295°K, free-carrier-absorption results, the shape of the interband optical absorption edge, and the room-temperature Seebeck coefficient.

CRYSTALLOGRAPHY AND VIBRATIONAL STRUCTURE

Room temperature powder x-ray measurements show a cubic perovskite structure for $KTaO_3$ with a lattice constant of 3.989 Å[21] The dielectric data presented below suggest that $KTaO_3$ remains essentially paraelectric and cubic to at least 4.2°K. Electron-spin-resonance results[22] are in agreement with this conclusion. Other experiments[23,24] reveal very small distortions from cubic symmetry at 4.2°K. These distortions are not understood, but may be associated with growth related strains. In any case $KTaO_3$ does not exhibit a transition to a ferroelectric phase over the temperature range of this investigation nor does $KTaO_3$ exhibit a transition to a significantly noncubic and nonferroelectric phase of the type observed in $SrTiO_3$ below 108°K.[25]

Because $KTaO_3$ is strongly polar, the dominant electron-lattice interaction is expected to involve longitudinal optical phonons. The cubic perovskite lattice contains five atoms in a unit cell so there are 15 vibrational degrees of freedom. Twelve of the associated vibrational modes belong to the optical branch.[26] Six of these are doubly degenerate transverse infrared active. These have been observed by Miller and Spitzer at 18.2, 50.3, and 117.5 μ.[27] The longitudinal polar-mode frequencies can be estimated from the zeros of the real part of the dielectric constant if damping shifts are neglected.[28] With this assumption the longitudinal modes are estimated to be at 11, 23, and 52 μ in $KTaO_3$. Eagles[29] has recently suggested that maximum electron coupling should be to the highest frequency longitudinal mode in rutile.

SAMPLE PREPARATION AND NATURE OF DONORS

$KTaO_3$ single crystals were grown in a platinum crucible by a modified Kyropolis method from a melt consisting of Ta_2O_5 and a 19% stoichiometric excess of K_2CO_3. Details are described elsewhere.[22] Crystal growth takes place onto a rotating seed as the melt is cooled at 3.5°C/h between approximately 1220 and 1120°C. When grown in an oxygen atmosphere crystals are colorless and transparent and exhibit resistivities greater than 10^{10} ohm-cm. Growth in air, however, often produces pale blue to dark blue crystals with resistivities in the 0.02–0.8 ohm-cm range. The blue crystals are presumably slightly reduced although an attempt to reoxidize them at 1250°C proved unsuccessful. Oxygen diffusion rates may be too low. Colorless, high-resistivity crystals could be grown in an air atmosphere by adding several hundred ppm SnO_2 to the growth melt. The compensating Sn^{4+} ions apparently act as deep electron traps.

It proved difficult to control the degree of crystal reduction possibly because of the variable degree of impurity compensation. Crystals having carrier concentrations in the range 3.5×10^{17}–1.5×10^{19} cm^{-3} were grown by pulling the crystal in approximately 1 mm steps every six hours during growth. This was found to give a layered crystal in which each layer was less reduced than the preceding one. Hall-effect samples were cut from these layers so as to minimize doping level variations within each wafer.

Reduction of insulating $KTaO_3$ crystals in hydrogen was attempted at 1000°C. The reaction rate was very slow, however, and only a very thin surface layer appeared to be affected after several hours exposure.

Because the static dielectric constant of $KTaO_3$ is large ($\kappa=243$ at 295°K), a simple hydrogen-like donor model predicts a very small donor ionization energy

[14] P. Kofstad, J. Electrochem. Soc. **109**, 776 (1962).
[15] P. Kofstad, Chem. Phys. Solids **23**, 1571 (1962).
[16] P. Kofstad, Chem. Phys. Solids **23**, 1579 (1962).
[17] R. F. Jannisch and D. H. Whitmore, J. Chem. Phys. **37**, 2750 (1962).
[18] P. Kofstad and D. J. Ruzicka, J. Electrochem. Soc. **110**, 181 (1963).
[19] F. T. Morin, J. Appl. Phys. Suppl. **32**, 2195 (1961).
[20] C. W. Nelson, Technical Report 179, Laboratory for Insulation Research, MIT, 1963 (unpublished).
[21] P. Vousden, Acta Cryst. **4**, 373 (1951).
[22] S. H. Wemple, thesis MIT, 1963 (unpublished).
[23] J. Geusic, S. Kurtz, T. Nelson, and S. Wemple, J. Appl. Phys. Letters **2**, 185 (1963).
[24] L. Bennett and J. Budnick, Phys. Rev. **120**, 1812 (1960).
[25] L. Rimai and G. A. De Mars, Phys. Rev. **127**, 702 (1962).
[26] V. Dvorak, Phys. Status Solidi **3**, 2235 (1963).
[27] R. C. Miller and W. G. Spitzer, Phys. Rev. **129**, 94 (1963).
[28] A. S. Barker, Jr., Phys. Rev. **132**, 1474 (1963).
[29] D. M. Eagles (to be published).

($\approx 10^{-4}$ eV). In addition, for $\kappa \geq 243$, the radius of a 1*S* donor orbital is comparable with the average spacing between donor centers (40–140 Å) so that an impurity band might be formed which could overlap the conduction band. We might therefore expect that carrier freeze-out would not occur at even the lowest temperatures. This is indeed observed as discussed below.

DIELECTRIC PROPERTIES

Figure 1 shows the temperature dependence of the static dielectric constant of $KTaO_3$. Significant deviations from Curie-Weiss law behavior are evident. The rounding-off below 30°K can be attributed at least partially to quantum effects.[30] The data above 30°K can be fitted to the following expression:

$$\kappa = 48 + [5.7 \times 10^4/(T-4)].$$

The large temperature-independent term may be qualitatively understood using the analysis of Silverman and Joseph.[31] The extrapolated Curie temperature is 4 ± 2°K; however, no hysteresis loops are observed to 1.6°K. Previously published data of Hulm, Matthias, and Long[32] show a Curie temperature of 13°K for $KTaO_3$. Impurities are probably causing this discrepancy since it is known that sodium[33] and niobium[34] raise the Curie temperature while iron[22] lowers it. Spectrochemical analysis of our samples shows <50 ppm Na, <300 ppm Nb, and <50 ppm Fe. Consequently, it is felt that the true "Curie temperature" of pure $KTaO_3$ is less than 1.6°K and that, in fact, a ferroelectric phase may not exist.

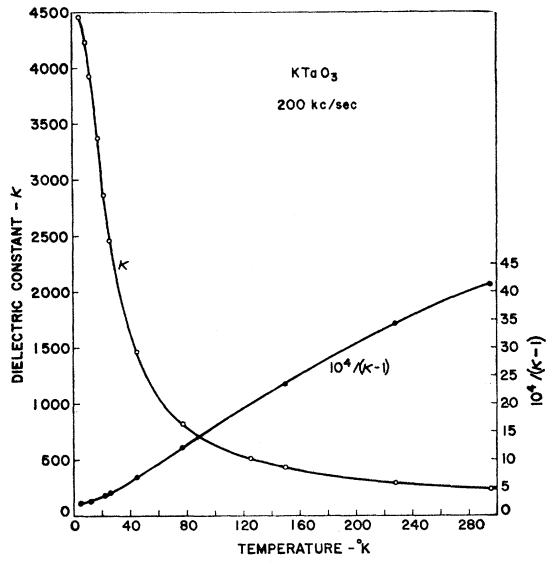

FIG. 1. Dielectric constant and reciprocal susceptibility of $KTaO_3$ as a function of temperature. Test frequency is 200 kcps.

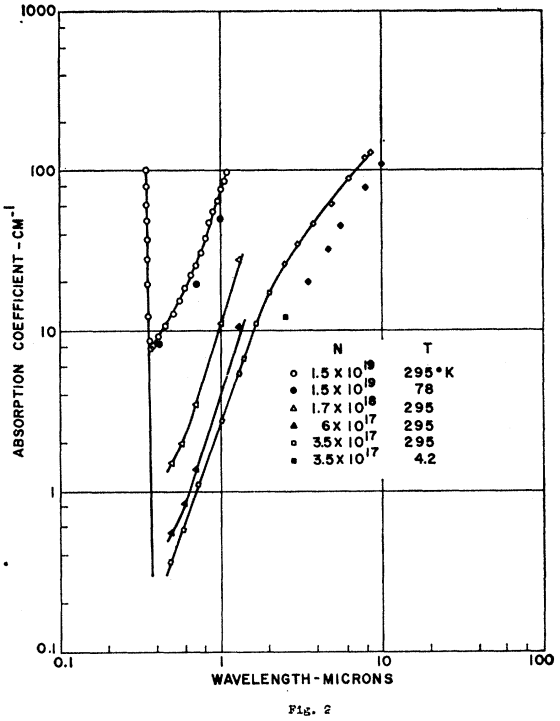

FIG. 2. Absorption coefficient of $KTaO_3$ as a function of wavelength.

The large static dielectric constant of $KTaO_3$ is expected to affect transport properties, particularly at low temperatures, because of polarization shielding of charged impurity or ionized donor scattering centers. Such shielding effects are contained explicitly in the Brooks-Herring[35] and Mansfield[36] ionized impurity scattering theories. The relevance of the static dielectric constant to these theories has been discussed by Kohn.[37]

OPTICAL PROPERTIES

Free-carrier optical absorption causes semiconducting crystals of $KTaO_3$ to appear blue. The lightly doped samples ($N < 10^{18}$ cm^{-3}) are pale blue and transparent, whereas the more heavily doped ones ($N > 10^{19}$ cm^{-3}) are dark blue. The wavelength dependence of the free-carrier absorption is shown in Fig. 2. Corrections for surface reflections at short wavelengths ($\lambda < 1\mu$) have been made using the refractive index (n) data of Fig. 3. These data were obtained from beam deflection measurements on a $KTaO_3$ prism. In the intermediate wavelength range ($1\mu < \lambda < 5\mu$), where the surface correction is small, we have taken $n = 2.2$, and for $\lambda > 5\mu$, a correction for lattice band absorption has been included. The main feature of Fig. 2 is the expected increase in

[30] J. H. Barrett, Phys. Rev. **86**, 118 (1952).
[31] B. D. Silverman and R. I. Joseph, Phys. Rev. **129**, 2062 (1963).
[32] J. K. Hulm, B. T. Matthias, and E. A. Long, Phys. Rev. **79**, 885 (1950).
[33] A. Linz (private communication).
[34] S. Triebwasser, Phys. Rev. **114**, 63 (1959).
[35] H. Brooks, Advances Electron. Electron Phys. **7**, 85 (1955).
[36] R. Mansfield, Proc. Phys. Soc. (London) **B69**, 76 (1956).
[37] W. Kohn, Chem. Phys. Solids **8**, 45 (1959).

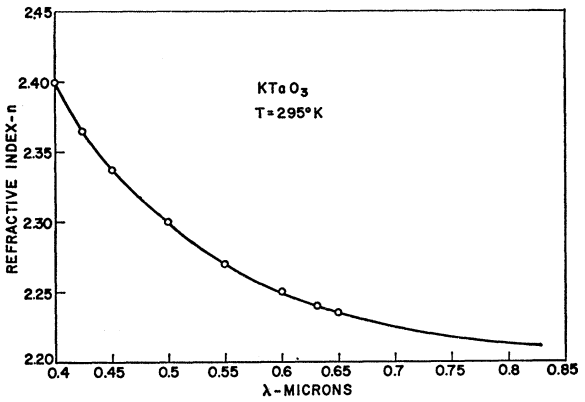

FIG. 3. Refractive index of $KTaO_3$.

absorption with increasing wavelength. The sharp increase in absorption near 3500 Å is the interband absorption edge. That the absorption in the infrared is indeed due to free carriers is shown in Fig. 4 where an approximately linear relationship between absorption coefficient and carrier concentration is indicated.

In the least heavily doped sample ($N=3.5\times10^{17}$ cm^{-3}), for $\lambda<2\mu$, we find that the absorption coefficient is proportional to $\lambda^{2.7\pm0.1}$. This is in fair agreement with the polar-mode-scattering free-carrier absorption theories of Visvanathan[38] and Feynman *et al.*,[39] which predict a $\lambda^{2.5}$ dependence provided $\omega\gg\omega_l$ where ω is the light frequency and ω_l is the nearest longitudinal lattice mode frequency. The more heavily doped samples, according to Fig. 2, exhibit a somewhat more rapid

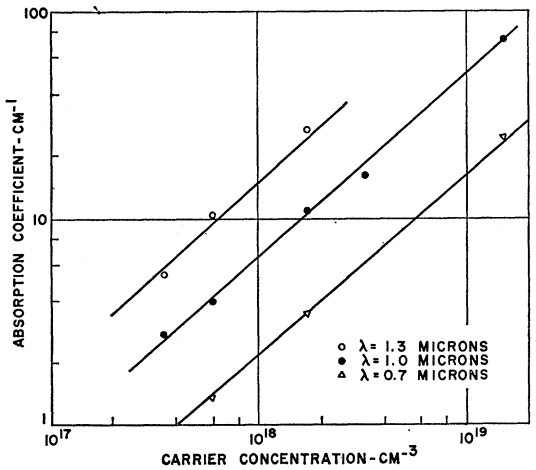

FIG. 4. Free-carrier absorption coefficient as a function of carrier concentration.

[38] S. Visvanathan, Phys. Rev. **120**, 376, 379 (1960).

[39] R. P. Feynman, R. W. Hellwarth, C. K. Iddings, and P. M. Platzman, Phys. Rev. **127**, 1004 (1962). This reference contains the results attributed to it in this section implicitly rather than explicitly by way of certain asymptotic expansions. Dr. Platzman has kindly made these results available to the author prior to publication.

absorption increase (absorption $\propto\lambda^3$). The λ^3 dependence is expected[38] if ionized-donor scattering predominates so that it is tempting to make the reasonable suggestion that the ionized-donor scattering probability is increasing with increasing carrier concentration. This possibility is not supported by the mobility data which show a room temperature Hall mobility which is independent of carrier concentration to at least 1.5×10^{19} cm^{-3}.

The limited long-wavelength data ($\lambda>2\mu$) of Fig. 2 show a less rapid wavelength dependence than at shorter wavelengths. This result is in agreement with the polar-mode free-carrier-absorption theory of Feynman, Hellwarth, Iddings, and Platzman[39] which predicts the following wavelength dependence provided $\omega>\omega_p$ and $\lambda>\lambda_l$:

$$A=\frac{4\pi}{3}\frac{\alpha}{n\lambda_l}\left(\frac{\omega_p}{\omega_l}\right)^2\left(\frac{\lambda}{\lambda_l}\right)^{2.5}\left(1-\frac{\lambda}{\lambda_l}\right)^{1/2}f\left(\frac{\hbar\omega_l}{kT}\right). \quad (1)$$

In Eq. (1), λ is the radiation wavelength; λ_l is the wavelength corresponding to the longitudinal polar mode frequency ω_l; ω_p is the "vacuum" plasma frequency given by $\omega_p^2=4\pi Ne^2/m^*$; N is the free-carrier concentration; m^* is a suitably averaged effective mass; n is the refractive index applicable at the wavelength λ; α is the electron-polar-mode coupling coefficient; and e is the electronic charge. The temperature dependence is contained in the function $f(\hbar\omega_l/kT)$. For $\hbar\omega_l/kT\gg1$, $f=1$. Assuming that electrons couple primarily to the longitudinal polar mode at $\lambda=11\mu$, the rounding off above 2μ in Fig. 2 is fairly well described by Eq. (1). That maximum coupling should be to the highest frequency longitudinal mode is reasonable since this mode has as its transverse counterpart the very strong lowest frequency transverse mode.[27] Eagles has recently shown[29] by detailed calculation that maximum electron coupling is to the highest frequency polar mode in rutile.

From Eq. (1) we can calculate the magnitude of A by substituting $N=3.5\times10^{17}$ cm^{-3}, $\lambda_l=11\mu$, and $m^*=0.8\,m_0$. This value of the effective mass is based on Seebeck effect measurements presented in the next section. The appropriate refractive index (n) to be substituted into Eq. (1) can be calculated using the reflectivity data of Miller and Spitzer.[27] The result is that n falls from 2.2 at $\lambda=1\mu$ to approximately 1.4 at $\lambda=10\mu$. Substituting into Eq. (1) we obtain for $\lambda=1\mu$, $A\approx0.2\,\alpha f$. Since $\hbar\omega_l/kT\approx5$ at room temperature, the factor f is approximately one. Using the Fröhlich formula[1] the coupling coefficient α is estimated to be two so that we obtain finally $A\approx0.4$ cm^{-1} which is in order of magnitude agreement with the observed value of 2.3 cm^{-1}. For $\lambda=10\mu$ the calculated value of $A=67$ cm^{-1} compares with the observed value of approximately 150 cm^{-1}. A major source of error in the above calculation may be our use of a single effective mass of $0.8\,m_0$. Recently Dr. G. Smith of these laboratories has observed cyclotron resonance in $KTaO_3$ at 1.4°K and

found an anisotropic effective mass with a mean value near 0.5 m_0. This anisotropy may significantly affect both ω_p and α in Eq. (1). In addition, the rather limited temperature dependence data shown in Fig. 2 suggest that there may be some coupling to modes for which the inequality $\hbar\omega_l/kT \gg 1$ does not hold.

To summarize, the free-carrier-absorption data for $KTaO_3$ are in fair agreement with polar-mode scattering theory. Very different results have been reported in semiconducting $SrTiO_3$ in which a broad band centered at approximately 1.4μ and also a weaker band at 0.43μ have been observed.[40] The differing free-carrier behavior of $KTaO_3$ and $SrTiO_3$ suggests that the band structures of these two isostructural materials may be quite different.

In addition to the free-carrier-absorption effects, Fig. 2 shows a sharp increase in absorption near 3500 Å associated with the interband absorption edge. A more detailed plot of the edge data both for a nonconducting ($\rho \approx 10^{10}$ ohm-cm) and a heavily doped sample ($N = 1.5\times10^{19}$ cm^{-3}) is shown in Fig. 5. In the nonconducting sample the absorption edge appears to be of the exponential type discussed by Urbach[41] although it should be emphasized that an absorption-edge tail can result from small traces of impurities present in the lattice, particularly transition metals. Unfortunately the band-edge data do not allow assignment of the conduction-band minimum to either $k=0$ or $k\neq0$. From these data we have assigned a band gap of 3.5 eV to $KTaO_3$. A peak in the photoconductivity response has been observed at 3.58 eV. The band-edge data for the heavily doped sample show a band gap slightly less ($\approx$0.025 eV) than for the undoped sample and also a strong tail. This tail may result from an impurity band contribution to the density of states near the conduction band edge in addition to free carrier absorption. Some tailing off of the absorption near the band edge is evident in Fig. 2 for even the more lightly doped samples.

SEEBECK EFFECT

The room-temperature Seebeck coefficient has been measured in a sample having $N = 3.5\times10^{17}$ cm^{-3} carriers. The result ($Q = 550$ $\mu V/°C$) allows calculation of an effective mass (m^*) from the expression $Q = 86[(\xi/kT)+A]\mu V/°C$ where ξ is the Fermi energy relative to the conduction band edge, and A is a constant which depends on the scattering mechanism and lies between 2 and 3 for polar-mode lattice scattering.[1] We can therefore calculate ξ and m^*. The result for $KTaO_3$ is $m^* = (0.8\pm0.28)m_0$. The above effective-mass estimate compares with $(14\pm2)m_0$ obtained on $SrTiO_3$ at room temperature by Frederikse *et al.*[6] The smaller effective mass in $KTaO_3$ than in $SrTiO_3$ is consistent with the larger orbital overlap expected in a 5*d* band.

[40] H. W. Gandy, Phys. Rev. **113**, 795 (1959).
[41] F. Urbach, Phys. Rev. **93**, 1324 (1953).

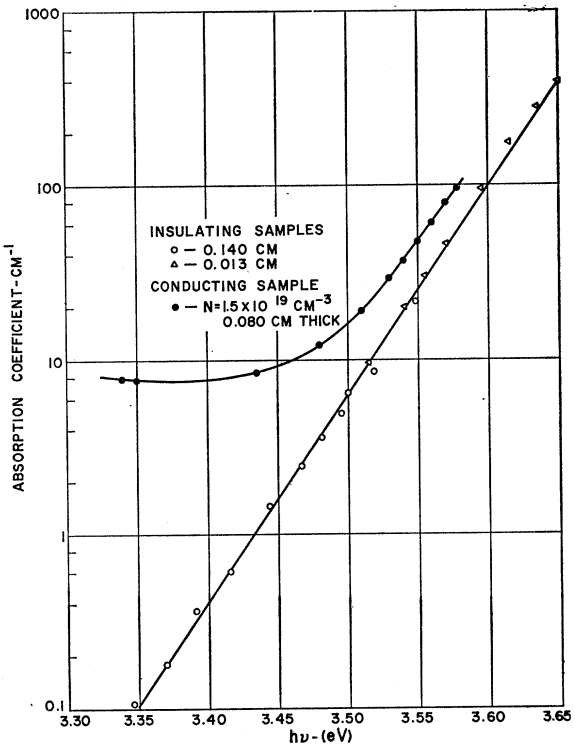

FIG. 5. Absorption coefficient versus wavelength near interband edge for semiconducting and insulating samples of $KTaO_3$.

HALL-EFFECT AND CONDUCTIVITY RESULTS

The dc Hall-effect and electrical-conductivity data were obtained using the four-arm "iron cross" sample shape described by van der Pauw.[42] Large contact arms minimize electrode effects, and the symmetric shape permits the use of small samples to that thermal effects are also minimized. Expressions relating the observed voltages to electrical conductivity and Hall coefficient are given by van der Pauw. The 5-mm-diam samples were cut from approximately 0.7-mm-thick slabs of $KTaO_3$ with a cavitron cutter. Electrical contact to the four arms was made with indium-gallium electrodes which were mechanically rubbed onto the sample. Preliminary etching in hydrofluoric acid significantly reduced the contact resistance although all traces of rectification could not be eliminated. Contact resistances (zero signal limit) were found to range from several hundred to only a few ohms. The lightly doped samples exhibited the larger values. Contact resistance was found to decrease continuously on cooling to liquid-helium temperature. No false nulls or bridge balancing difficulties were encountered. All Hall and conductivity voltages were measured with an L&N Type-K3 potentiometer. Conventional current and field reversal procedures were used to minimize thermal effects and electrode misalignment errors. The sample was mounted

[42] L. J. van der Pauw, Philips Res. Repts. **13**, 1 (1958).

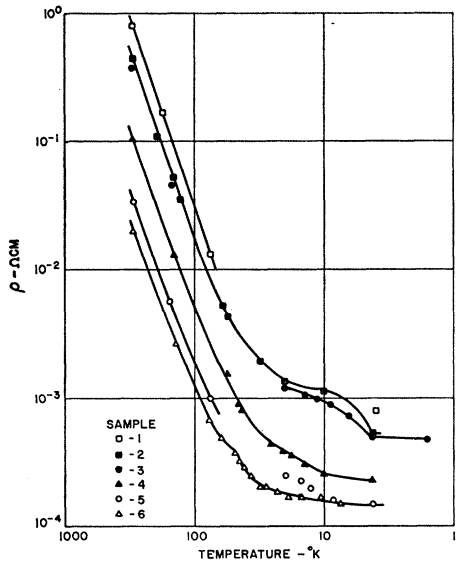

FIG. 6. Electrical resistivity as a function of temperature.

within a copper heat shield, and contact to the In-Ga electrodes was made with phosphor bronze springs. Temperatures were measured with a copper-constantan thermocouple placed adjacent to the sample. A Varian 12-in. magnet capable of providing 12-Kg fields was used for all measurements.

The electrical conductivity results are shown in Fig. 6. Complete temperature dependences were not obtained for all the samples. There is no indication in Fig. 6 of carrier freeze-out, and at low temperatures electrical conductivities are remarkably high. A more thorough discussion of these data will be given after presenting the Hall-effect results.

The dc Hall coefficient R was found to be almost independent of temperature over a range extending from room temperature to 4.2°K and to 1.6°K in one sample. The slight temperature dependence was in the direction of lower R at low temperatures. This is shown in Table I in which are tabulated room temperature and 4.2°K values.

Values of the carrier concentration in Table I were calculated from the 4.2°K Hall coefficient using the expression $R=-1/Ne$. In general, $R=-AB/Ne$ where A is a constant which depends on the scattering mechanism and the degree of degeneracy, and B depends on the band shape—e.g., spherical, many-valley, etc. In the degenerate limit $A=1$. As discussed below all of our samples are degenerate at 4.2°K so that N can be readily calculated at this temperature if we also arbitrarily assume that $B=1$ as for a spherical band. A value of B equal to 0.326 has been reported[43] for the many-valley band of Bi_2Te_3 so that our assumption that $B=1$ could result in concentrations as much as a factor of three too high. To check this possibility an independent measure of the carrier concentration has been obtained from the bias dependence of the capacitance of Au-$KTaO_3$ Schottky surface barrier diodes[44] for which

$$1/C^2=(2/qN\kappa A^2)(V_D+V_B). \tag{2}$$

C is the small signal differential capacitance about the bias point, qN is the assumed constant positive charge density in the depletion layer, κ is the static dielectric constant, A is the diode area, V_D is the diffusion potential, and V_B is the externally applied bias voltage. Diodes were formed on freshly cleaved [100] surfaces. The data for one sample are plotted in Fig. 7. From the intercept we obtain $V_D=1.6$ V, and from the slope we find $N=6\times10^{17}$ cm^{-3} in agreement with the concentration determined from Hall measurements. A value of $B=1$ is therefore reasonable. Additional surface barrier diode results including photothreshold measurements will be reported in a later publication.

Taking $B=1$ and $A=1$ at 4.2°K, the Hall-coefficient data of Table I suggest that $A=1.1$–1.2 at room temperature. Since lattice scattering predominates at room temperature as shown by the concentration independent mobility, we would expect $A=1.18$ if acoustic-mode scattering predominates and $A\approx1.1$ for polar-mode scattering.[45] The observed value of $A=1.1$–1.2 is not surprising, then, but the data do not distinguish between these two scattering mechanisms. We conclude that

TABLE I. Summary of Hall-effect results at 295 and 4.2°K.

Sample No.	Calculated N (cm^{-3})	R Hall coefficient-cm^3/Coul. (295°K)	(4.2°K)	μ_H Hall mobility-cm^2/V-sec (295°K)	(4.2°K)
1	3.5×10^{17}	20.3	18	27	23 000
2	6.0×10^{17}	12.9	10.4	29	19 000
3	6.6×10^{17}	11.5	9.4	31	19 000
4	2.4×10^{18}	3.0	2.6	30	11 000
5	7.8×10^{18}	1.0	0.80	30	5300
6	1.3×10^{19}	0.62	0.48	31	3400

[43] J. R. Drabble, R. D. Groves, and R. Wolfe, Proc. Phys. Soc. (London) **71**, 430 (1958).
[44] H. K. Henisch, *Rectifying Semiconductor Contacts* (Oxford University Press, New York, 1957).
[45] B. F. Lewis and E. H. Sondheimer, Proc. Roy. Soc. (London) **A227**, 241 (1955).

no carrier freezout occurs for concentrations as low as 3.5×10^{17} cm^{-3}, and that the small temperature dependence of R probably results from changes in the scattering mechanism and/or degree of degeneracy.

The room-temperature Hall mobility ($R\sigma$) of 30 cm^2/V-sec in $KTaO_3$ compares with 6 cm^2/V-sec in $SrTiO_3$ [6] and somewhat lower values in rutile.[7] The higher value in the 5*d* tantalate than in the 3*d* titanates is in line with the claim that a 5*d* band should be broader than a 3*d* band and is consistent with the lower Seebeck effective mass previously discussed. The effect of 5*d* overlap apparently more than compensates for the somewhat larger lattice constant of $KTaO_3$.

The temperature dependence of the Hall mobility is plotted in Fig. 8. These data show a T^{-3} dependence above approximately 100°K where the Hall mobility is independent of carrier concentration. Lattice scattering clearly dominates at these temperatures. The experimental results can be fitted to the following expression:

$$\mu_H=8\times10^8T^{-3}\ \text{cm}^2/\text{V-sec}. \tag{3}$$

The above result is not in agreement with the usual polar-mode or acoustic-mode lattice scattering theories although the same T^{-3} dependence is observed in $SrTiO^3$.[6] The T^{-3} dependence in $KTaO_3$, $SrTiO_3$, and other polar semiconductors as well[46] is not understood at present although it could conceivably arise from mixtures of polar mode, acoustical mode, and many-valley scattering.

TABLE II. Calculated degeneracy transition region ΔT for three different carrier concentrations.

Sample No.	N	$(m^*/m_0)\Delta T$ °K
2	6.0×10^{17}	8–30
4	2.4×10^{18}	19–73
6	1.3×10^{19}	58–220

Below 100°K the Hall mobility results of Fig. 8 show a concentration dependence resulting from impurity or ionized donor scattering. An important consideration regarding these low-temperature data is the question of degeneracy. A reasonable definition of the transition region between a predominately nondegenerate and a predominately degenerate semiconductor is given by the inequality $0<\xi/kT<4$, where ξ is the Fermi-level distance above the conduction band edge. The above expression implies that $0.8<N/N_c<6$, where $N_c=4.82\times10^{15}T^{3/2}(m^*/m_0)^{3/2}$, N is the carrier concentration, and m^*/m_0 is a suitably averaged effective mass. The calculated transition region ΔT is given in Table II

[46] R. W. Ure, Jr., in *Proceedings of the International Conference on the Physics of Semiconductors, Exeter* (The Institute of Physics and the Physical Society, London, 1963), p. 659.

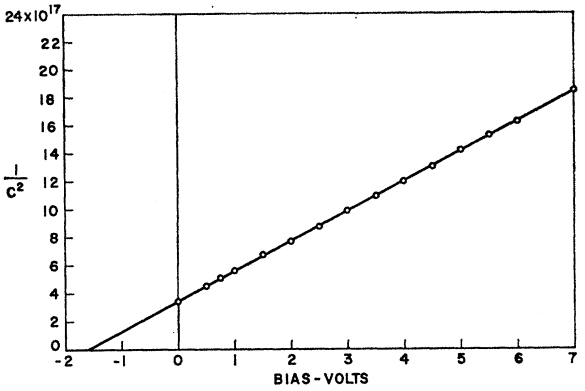

FIG. 7. Capacitance of Au-$KTaO_3$ surface barrier diode as a function of bias voltage. Diode area is 2×10^{-3} cm^2.

for several carrier concentrations. Assuming that $m^*\simeq m_0$ the transition regions in Table II over which the electron statistics are expected to change are close to the positions of the humps in the curves for samples 2, 4, and 6 in Figs. 6 and 8. This suggests that these humps may be associated with a change of statistics. The doubling of mobility in sample 2 between 10 and 4.2°K is particularly striking.

At 4.2°K all of our $KTaO_3$ samples are expected to be degenerate. The degenerate impurity scattering formula of Mansfield[36] is

$$\mu=3h^3\kappa^2N/16\pi^2e^3Z^2m^{*2}N_If(x), \tag{3}$$

where

$$x=\tfrac{1}{2}(h/e)^2(\kappa/m^*)(3N/8\pi)^{1/3}, \tag{4}$$

and $f(x)=\ln(1+x)-x/1+x$. N is the carrier concentration, N_I is the concentration of scattering centers with charge Z, and κ is the static dielectric constant.

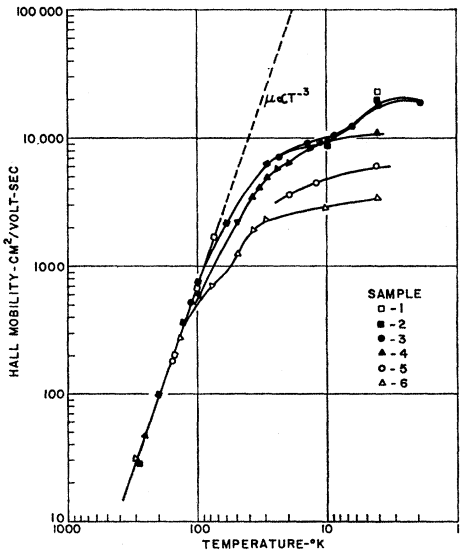

FIG. 8. Hall mobility as a function of temperature.

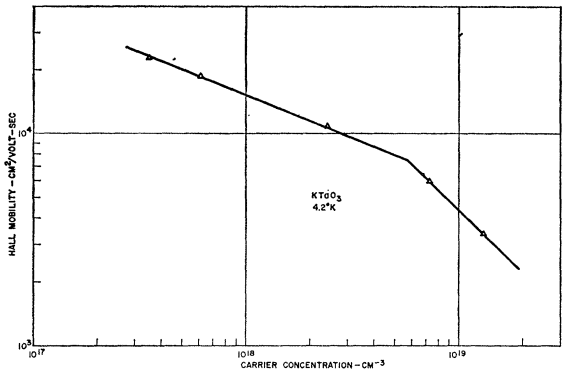

FIG. 9. Hall mobility as a function of carrier concentration at 4.2°K.

Taking $\kappa=4400$, $Z=2$, and $m^*=m_0$ we obtain

$$\mu\simeq\frac{10^5(N/N_I)}{\ln(10^{-4}N^{1/3})}\ \text{cm}^2/\text{V-sec}. \tag{5}$$

If $N=2N_I$ as for doubly ionized oxygen-vacancy donors, the following results are obtained. Calculated mobility values in Table III are somewhat too high. The factor-of-2 discrepancy at low concentrations may result from the fact that $N\neq 2N_I$, but is somewhat less due to charged scattering centers associated with impurities (Sn^{4+}, Fe^{3+}, etc.). Charged-impurity concentrations of approximately 30 ppm would be required to reduce the calculated mobility by a factor of 2, and such concentrations are very likely present. It should be pointed out that the large mobility at low temperature in $KTaO_3$ appears to be a consequence of shielding of charged scattering centers by the large static dielectric constant.

The calculated mobility in Table III is a weaker function of carrier concentration than the observed mobility which is plotted as a function of concentration in Fig. 9. This discrepancy may arise from the smallness of the scattering cross section Σ. Allgaier and Houston[47] in their analysis of PbTe data suggest that Σ values of the order of the square of the lattice constant imply local cell interactions which cannot be treated by expressions involving averaged lattice properties such as κ. In the case of degenerate statistics these authors write the cross section Σ as follows:

$$\Sigma=\left(\frac{\pi}{3}\right)^{1/3}\frac{2e}{h}\frac{1}{N^{4/3}\mu}\ (\text{cgs}), \tag{6}$$

where N is the carrier concentration, μ is the mobility, and e is the electron charge. The values of Σ tabulated in Table III have been calculated from Eq. (6). Since the square of the lattice constant is approximately 16 (Å)², we expect mobility calculations based on Eq. (6) to be invalid if the calculated Σ turns out to be of this order. If the scattering cross section can in fact only reach some minimum value Σ_0 of the order of 16 (Å)², we find according to (6) that $\mu\propto N^{-4/3}/\Sigma_0$. The slope in Fig. 7 for high concentrations is approximately $-\frac{4}{3}$ which suggests that the constant scattering cross section model may be applicable. Table III gives $\Sigma_0\simeq 50$ (Å)². This area corresponds to a two-unit-cell square and is a reasonable value for the minimum scattering cross section.

[47] R. S. Allgaier and B. B. Houston, Jr., in *Proceedings of the International Conference on the Physics of Semiconductors, Exeter* (The Institute of Physics and the Physical Society, London, 1963), p. 172.

TABLE III. Calculated mobilities and scattering cross sections for various carrier concentrations at 4.2°K.

N cm^{-3}	Mobility cm²/V-sec Calculated	Observed	Scattering cross section (Å)²
3.5×10^{17}	47 000	23 000	850
6.0×10^{17}	45 000	19 000	500
2.4×10^{18}	41 000	11 000	136
7.8×10^{18}	38 000	5300	58
1.3×10^{19}	37 000	3400	47

Ure[46] has called upon a two-band model to explain a break point similar to that of Fig. 9 in bismuth telluride data at 4.2°K. Our data do not permit an unambiguous choice between this model and the constant scattering-cross-section model. However, the reasonable value of Σ_0 which we obtain seems rather convincing evidence for the latter model.

DISCUSSION

Electron conduction in oxygen deficient $KTaO_3$ exhibits several features of interest. Effective-mass estimates are lower, and mobilities are higher than in the isostructural perovskite $SrTiO_3$. Mobilities and conductivities are remarkably large for a d-band oxide semiconductor reaching values of 23 000 cm²/V-sec and 8×10^3 (ohm-cm)$^{-1}$ at 4.2°K. The larger mobility (and lower effective mass) in $KTaO_3$ than in $SrTiO_3$ is consistent with the expected larger overlap of $5d$ orbitals compared with $3d$. Band calculations for $KTaO_3$ have not as yet been attempted however. In the lattice scattering region above 100°K both $KTaO_3$ and $SrTiO_3$ exhibit Hall mobilities having a power-law dependence of the form $\mu_H\propto T^{-3}$ which suggests strong similarities in scattering. Free-carrier-absorption results are quite different, however, only the $KTaO_3$ data being indicative of polar-mode lattice scattering.

ACKNOWLEDGMENTS

It is a pleasure to acknowledge helpful discussions with P. M. Platzman, A. S. Barker, Jr., S. K. Kurtz, and D. Kahng. Thanks are also due R. Wolfe for the Seebeck measurements, and Miss D. Dodd for some of the free-carrier-absorption measurements. Thanks are also extended to A. Linz and W. Belruss of the Laboratory for Insulation Research, MIT.